Chemical Engineering Journal 237 (2014) 352–361

Contents lists available at ScienceDirect

Chemical Engineering Journal

journal homepage: www.elsevier.com/locate/cej

Chitosan–clay composite as highly effective and low-cost adsorbent for batch and fixed-bed adsorption of methylene blue

M. Auta [a,c], B.H. Hameed [a,b,*]

[a] School of Chemical Engineering, Engineering Campus, Universiti Sains Malaysia, 14300 Nibong Tebal, Penang, Malaysia
[b] Chemical Engineering Department, College of Engineering, King Saud University, P.O. Box 800, Riyadh 11421, Saudi Arabia
[c] Department of Chemical Engineering, Federal University of Technology, Minna, Nigeria

HIGHLIGHTS

- Modified Ball clay was coalesced with chitosan to form composite adsorbent (MBC–CH).
- MBC–CH gave high adsorption of methylene blue in batch and fixed-bed systems.
- MBC–CH activity can be sustained on the event of adsorption system failure.
- MBC–CH can be regenerated and reused in many cycles of adsorption with resilience.

ARTICLE INFO

Article history:
Received 29 June 2013
Received in revised form 13 September 2013
Accepted 16 September 2013
Available online 15 October 2013

Keywords:
Methylene blue
Adsorption
Regeneration
Modeling
Chitosan–clay composite

ABSTRACT

Modified Ball clay (MBC) and chitosan composite (MBC–CH) was prepared and its application for methylene blue (MB) adsorption from aqueous solution in an industrial prototype fixed-bed column adsorption was investigated. Morphological structure and functional groups of the MBC–CH were determined by scanning electron spectroscopy and Fourier transform infrared spectroscopy analysis, respectively. Batch adsorption studies revealed that MB adsorption on MBC–CH increased with increase in initial concentration and solution pH 4–12. Study on effect of some inorganic salts on MB adsorption revealed that sodium sulphate anions (SO_4^{2-}) had greater inhibition effect than those of sodium chloride and sodium bicarbonate on both MBC and MBC–CH. The effects of initial concentration (30–300 mg/L), adsorbent bed height (2.5–4.5 cm) and influent flow rate (5–10 mL/min) on fixed-bed column adsorption breakthrough curves were evaluated. Column sorption capacities were 70 mg/g for MBC and 142 mg/g for MBC–CH. Dynamic modeling analysis revealed that Bohart–Adams model can best be used to predict the effluent breakthrough curves for successful design of MB adsorption than Yoon–Nelson model. Adsorption system failure studies showed that the adsorbents were resilient with some improvement observed at time of exhaustion and increased volume of effluent treated. The MBC–CH had above 50% adsorption uptake capacity after five regeneration cycles, this was higher than MBC. Adsorption of MB on MBC–CH was spontaneous, endothermic and had great affinity between the adsorbate and adsorbent. The findings of this study revealed that MBC–CH is a potential adsorbent for cationic dye pollution remediation.

1. Introduction

Conventional batch adsorption is widely used in laboratory experiments to assess adsorption capacity of adsorbents and to generate design data for large scale systems; however, it can only be used to treat small volume of wastewater and as such is not popular in industrial applications [1–3]. Fixed-bed adsorption system is commonly used for gas and liquid pollution control. It is designed in such a way that the flowing polluted fluid comes in contact with a fixed amount of adsorbent thereby creating room for treatment of large volume of effluent fluid with less monitoring requirement [4]. The system is simple to operate, low cost and can easily be scaled up [5].

Several alternative low cost adsorbents have been developed from minerals, agricultural and industrial waste materials amongst others. These adsorbents applicability for treatment of dye and heavy metals wastewaters, gas and pharmaceutical wastes pollution and oil spillage control have been investigated. Clay minerals application in pollution control has received gross attention over

* Corresponding author at: School of Chemical Engineering, Engineering Campus, Universiti Sains Malaysia, 14300 Nibong Tebal, Penang, Malaysia. Tel.: +64 05996422; fax: +60 45941013.
E-mail address: chbassim@eng.usm.my (B.H. Hameed).

1385-8947/$ - see front matter © 2013 Elsevier B.V. All rights reserved.
http://dx.doi.org/10.1016/j.cej.2013.09.066

the past decades. Modification of clay through acid treatment, calcinations, functionalization and pillaring are among several ways that effort has been made by researchers to enhance its usability beyond its application in natural form [6]. Chitosan is a biopolymer derived from N-deacetylatilation of chitin which is found in abundance naturally. The high content of hydroxyl and amino functional groups of chitosan are potentials that has been harnessed in the field of adsorption of substances [7]. However, chitosan has some mechanical and chemical deficiency challenges which when improved upon, increases its adsorption capability [8,9].

Integration of an adsorbent with other materials through methods such as grafting, impregnation, chelation and crosslinking has better adsorption properties than the individual components effects [10]. The synergy of adsorbent materials as composites have been tailored for gas, metals, pharmaceutical wastes, dyes and pesticide remediation. Composite adsorbents can be prepared with the sole aim of enhancing their selectivity, regeneration, surface area, mechanical strength and surface chemistry amongst others [11,12].

Among classes of dyes, the cationic dyes are commonly used for different purposes due to their ease of applicability, durability, and good fastness to materials; however, their demerit effects are immense. Cationic dyes are known to have carcinogenic, mutagenic and high coloring effects on the entire ecosystem when discharged as waste in the environment [13]. Methylene blue (MB) a cationic dye has very wide applications which make it one of the common pollutants or constituent of color effluents. Several attempts have been made by previous researchers to address MB health effect as a pollutant in wastewater through the development and application of different adsorbents for its uptake [14–17].

In continuation with the exploration of effective MB pollution mitigating measure which has been the bane of researchers towards ensuring sustainability of serene environment, potentials of local clay in Malaysia for industrial application as adsorbent was investigated in this research. The modified Ball clay (MBC) previously reported [18] was composited with chitosan for adsorption of MB in a fixed-bed column. Behavior of breakthrough curves was studied through variation of the MB influent initial concentration, bed height and solution flow rate. The fixed-bed column adsorption was modeled with Bohart–Adams and Yoon–Nelson models. The use of some various salts in the textile industries to improve color fastness was investigated through studying effect of some inorganic salts on adsorption, and the adsorbent reusability test was conducted through desorption studies.

2. Materials and methods

Chitosan flakes ((molecular weight, MW = 400,000 Da, degree of deacetylation, DD = 90%) was obtained from Hunza Pharmaceutical Sdn Bhd., Nibong Tebal, Malaysia. Aluminum hydroxide ($Al(OH)_3$), sodium hydroxide (NaOH), sulfuric acid (H_2SO_4) and acetic acid (CH_3COOH) were purchase from Merck chemical company, while methylene blue (MB) was obtained from Sigma–Aldrich Chemicals, Malaysia. Ball clay was locally sourced in Malaysia. Schematic structure of methylene blue and its properties are shown in Scheme 1.

Name of dye	Methylene blue
Molecular formula	$C_{16}H_{18}N_3SCl$
Molecular weight (g/mol)	319.85
Methylene blue purity (%)	≥85
Maximum wavelength λ (nm)	668
Chemical structure	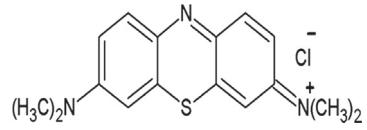

Scheme 1.

2.1. Preparation of MBC–CH adsorbent

The procedure for preparation of modified Ball clay (MBC) is as reported in our previous work [18]. Chitosan (1 g) was dissolved in 52 mL of 0.7 M acetic acid, and then 1 g of MBC (powder MBC prior to mixing with sodium alginate to form beads) was added and stirred for 24 h. The mixture was drop-wisely transferred to 0.67 M NaOH solution to form beads and was freeze dried. The freeze dried beads MBC–CH) were crushed into particle sizes of 0.5–2.0 mm and were tagged MBC–CH.

2.2. MBC–CH adsorbent characterization

Scanning electron microscope (EMJEOL-JSM6301-F) model and an Oxford INCA/ENERGY-350 microanalysis system was used for determination of MBC–CH morphological structure before and after adsorption of MB.

Perkin Elmer Spectrum GX Infrared Spectrometer with resolution of 4 cm^{-1} in the range of 2000–400 cm^{-1} was used for the FTIR analysis of MBC–CH. The MBC–CH adsorbent and potassium bromide (KBr) were dried in an oven and then ground together in a ratio of 20:1 (KBr:MBC–CH) for FTIR measurement using disc sample method.

2.3. Kinetic and equilibrium adsorption studies

Initial concentrations (30–300 mg/L) of 100 mL MB was put in a set of Erlenmeyer flasks where 0.1 g of MBC–CH was added. The flasks were place in water-bath shaker set at 140 rpm and 30 °C until equilibrium concentration between the adsorbent and solution was attained. Prior to equilibrium, kinetics of the adsorption process was studied by sampling the residual MB concentration in solution using UV–Vis spectrophotometer (Shimadzu UV/Vis 1601 spectrophotometer, Japan) at a maximum wavelength of 668 nm.

The adsorbent adsorbate uptake, q_t (mg/g) was evaluated as:

$$q_t = \frac{(C_o - C_t)_v}{w} \quad (1)$$

where C_o and C_t (mg/L) are the initial MB liquid-phase concentration and at any time t, respectively; V (L) is the volume of the solution; and W (g) is the mass of the MBC–CH. The entire process was repeated by varying water-bath shaker temperature to 40 and 50 °C.

In a similar manner as the equilibrium adsorption studies, about 0.5 and 1.0 M salts of NaCl, $NaHCO_3$ and Na_2SO_4 were added to the initial MB solution to study their effect on the adsorption process. The effect of solution pH 4–12 effect on MB adsorption was studied in the batch operation experiment by adding either 0.1 M of NaOH or HCl to adjust the initial pH.

2.4. Regeneration of adsorbent

Adsorbent recovered after batch equilibrium studies were rinsed mildly with distilled to remove residual dye particles and then dried. The dried adsorbent was placed in a stripping solution contained in 250 mL Erlenmeyer flask. The solution was 100 mL

distilled water adjusted to pH 4 using 0.1 M HCl. The flask was then placed in water bath shaker with settings as in Section 2.3 (Kinetic and equilibrium adsorption studies) to attain dynamic equilibrium. The adsorbent was recovered, dried and placed in a flask containing 100 mL of 200 mg/L initial solution of MB for the next equilibrium adsorption experiment. This cycle was repeated five times. The MB desorption and adsorption uptake were determined using Eq. (1).

2.5. Fixed-bed adsorption experiment

The experiment was conducted in a 1.2 cm diameter and 19.5 cm length encased Pyrex glass tube having an embedded stainless steel mesh for supporting layer of adsorbent. The MBC–CH 0.8, 1 and 1.2 g adsorbent corresponding to 2.5, 3.6 and 4.5 cm bed heights, respectively were measured into the column. Fluidization and bypass flow of the system were retarded by introducing some spherical glass beads on the mesh. Influent flow rate of 5, 8 and 10 mL/min in an upward direction with the aid of peristaltic pump (Master-flex, Cole-Parmer Instrument Co.) were used each for 50, 100 and 200 mg/L initial concentrations. An isothermal condition of the column was achieved by making a loop between it and water-bath set at 30 °C. The effluent MB concentration was measured at intervals at maximum MB wavelength, λ_{max} = 668 using UV–Vis spectrophotometer (Shimadzu UV/Vis 1601, Japan).

2.6. Fixed-bed column data analysis

The MB adsorption breakthrough profiles were obtained from C_t (mg/L) or C_t/C_o vs V_t (mL) or t (min) plots; where C_t is effluent concentration, C_o influent concentration, V_t volume of effluent treated and t is the service time. The treated effluent volume V_t is determined as:

$$V_t = Qt_e \tag{2}$$

where Q (mL/min) and t_e (min) are the influent flow rate and time of exhaustion.

Fixed-bed capacity q_{total} (mg) at set influent conditions (concentration and flow rate) is determined by computation of area under the plot from the integral of adsorbed concentrations expressed as C_{ad}($C_{ad} = C_o - C_t$) mg/L for a given time t (min) [19,20]:

$$q_{total} = \frac{QA}{1000} = \frac{Q}{1000}\int_{t=0}^{t=t_{total}} C_{ad}\,dt \tag{3}$$

where t_{total}, (min) is the total flow time, Q and A are the volumetric flow rate (mL/min) and the area under the breakthrough curve, respectively. The equilibrium uptake ($q_{eq(exp)}$) (mg/g) can be evaluated using Eq. (4) [21]:

$$q_{eq(exp)} = \frac{q_{total}}{m} \tag{4}$$

where m (g) is the mass of adsorbent in the column. Amount of adsorbate passed into the column-W_{total} (mg) is determined as:

$$W_{total} = \frac{C_o Q t_{total}}{1000} \tag{5}$$

The percentage adsorbate uptake is calculated as:

$$R\% = \frac{q_{total}}{W_{total}} \times 100 \tag{6}$$

2.7. Kinetic models of fixed-bed column adsorption

Bohart–Adams model which describes the initial part of a breakthrough profile is assumed to have rectangular shape isotherm [22]. The model equation can be expressed as:

$$\ln\left(\frac{C_o}{C_b} - 1\right) = \frac{k_{BA}N_oZ}{U} - k_{BA}C_o t_b \tag{7}$$

where C_o and C_b are the initial and breakthrough concentrations, k_{BA}(L/mg min) is Bohart–Adams model's constant, N_o is fixed-bed sorption capacity per unit volume (mg/L), Z (cm) is the bed height, U (mL/min) is the linear or superficial velocity and t_b (min) is the breakthrough time. The model's parameters are obtained from the intercept and slope of a linear plot of $\ln[(C_o/C_b) - 1]$ against t_b.

Yoon–Nelson kinetic model stands on the premise that the probability of adsorbate adsorption and adsorbate breakthrough on the adsorbent is proportional to the rate of decrease in the probability of adsorption of adsorbate molecule [23]. The model's equation for single component is given as:

$$\ln\left(\frac{C_t}{C_o - C_t}\right) = k_{YN}t - \tau k_{YN} \tag{8}$$

where k_{YN} (1/min) is the model's rate constant, τ (min) is the time required for 50% adsorbate breakthrough. The model's parameters k_{YN} and τ were obtained from the slope and intercept, respectively of plot of $\ln[C_t/(C_o - C_t)]$ against t.

2.8. Fixed-bed adsorption system failure studies

At about 50% to exhaustion (C_o/C_t) the system was switched off and then continued after 48 h and finally allowed to attain exhaustion. The system was operated at MBC and MBC–CH bed depth of 3.6 cm with MB influent concentration of 50 mg/L, 5 mL/min flow rate at 30 °C).

3. Results and discussion

3.1. Characterization of MBC–CH

The morphological structure of MBC–CH presented in Fig. 1 revealed by SEM analysis showed that the MBC particles were well dispersed on the chitosan surfaces, indicating a homogeneous combination of the constituents. Similar morphological images were viewed by previous researchers on chitosan clay composites [24].

Spectra of MBC–CH before and after adsorption of MB were examined for functional groups that contributed to the adsorption process; the spectrums are shown in Fig. 2. Vibrations of silica group comprising of Si—O—Si symmetric and asymmetric stretches, Si—O—Si bend and silanol Si—O stretches were found on 466–1120 cm^{-1} wavenumbers of MBC. The —NH_2 groups are common features in chitosan spectrums but their absence in MBC–CH spectrum revealed that the composite was successfully synthesized as they were used up during grafting or amino bonding (chitosan) with MBC [7,25]. Three points of symmetry of 500,

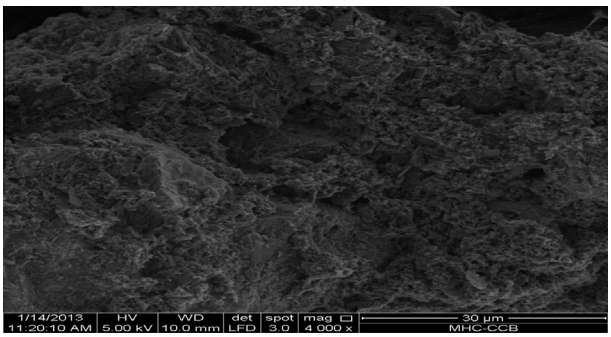

Fig. 1. The morphological structure of MBC–CH.

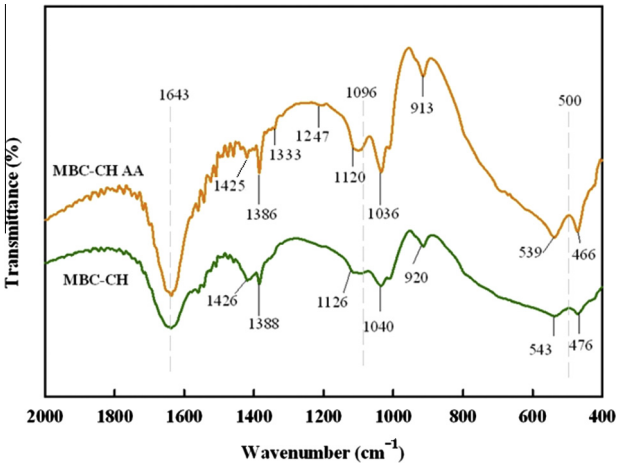

Fig. 2. The FTIR spectrums of MBC–CH before and after adsorption (MBC–CH AA) of MB.

1096 and 1643 cm^{-1} wavenumber were located on MBC–CH spectrums before and after adsorption of MB; presence of the strong peak on wavenumber 1643 cm^{-1} is a common characteristic of adsorption band of chitosan [26]. While the peaks on wavenumber 500 and 1096 cm^{-1} were attributed to silica (Si—O—Si) bend and asymmetric stretch, respectively [27]. The numerous and higher intensity of adsorption band peaks at various wavenumbers on MBC–CH than MBC [18] is attributed to the coalesced effect between the clay and chitosan. An oxygen containing functional group adsorption band at 1426 cm^{-1}spectrum (before adsorption) corresponding to stretching vibrations of the —COO^- was observed to have decreased on the spectrum after adsorption. The decrease in intensity was due to the extinction of some —COO^- used for adsorption of MB molecules [16]. Chitosan CH_3 symmetrical deformation was observed when the peak at 1388 cm^{-1} before adsorption moved to 1386 cm^{-1} after adsorption; shifting of sulfoxide (S═O) compound on 1040 cm^{-1} before adsorption to 1036 cm^{-1} after adsorption was also observed [28]. The peak at 1386 cm^{-1} also signified the C═C stretch of alkyl R– that indicated presence of MB molecule adsorbed [29]. Adsorption of MB on MBC–CH also resulted in vibration of O—H out-of-plane bend from 920 cm^{-1} before adsorption to 913 cm^{-1} after adsorption. Shifting and vibration of functional groups was observed on the spectrum of kaolin clay [30]. Some new peaks were detected on the MBC–CH spectrum after adsorption at 1333 and 1247 cm^{-1} for aromatic nitro compound and S═O stretching, respectively which were attributed to presence of MB molecules on the adsorbent surface [31]. The presence of more functional groups on MBC–CH composite as compared with MBC [18,25] adsorbent contributed to faster and higher adsorption of MB.

3.2. Effect of initial concentration on adsorption of MB

Profiles for MB uptake by MBC–CH at various initial concentrations are shown in Fig. 3. The presence of limited adsorbate molecules of lower initial concentration resulted in a greater percentage of MB uptake and faster attainment of equilibrium but contrarily, an opposite observation was made at higher initial concentrations (Fig. 3). This was attributed to numerous active sites on MBC–CH which outstripped the scanty molecules of adsorbates in low concentrations, and competition for limited actives for numerous adsorbate molecules at higher concentrations. But at any point in time, higher solute uptake was recorded at higher initial concentration of the adsorption experiments. Variation of initial

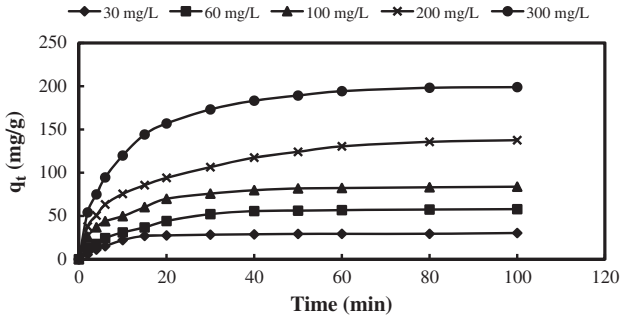

Fig. 3. Effect of initial concentration on MB adsorption (V = 100 mL, W = 0.10 g, shaking speed of 140 rpm, and temperature = 30 °C).

concentration from 30 to 300 mg/L gave a corresponding solute uptake of 26.93–193.23 mg/g. Similarly, increase in initial concentration was observed to increase the adsorption uptake of MB by previous researchers [32].

3.3. Effect of inorganic salt on MB adsorption

Adsorption of MB on both MBC and MBC–CH were affected by the inorganic salts in the solution. Graphical description of effect of the inorganic salts on MB adsorption on both adsorbents is presented in Fig. 4. Increase in the concentration of inorganic salts concentration (ionic strength) was observed to decrease the MB% adsorption removal. The effect was attributed to competition between the salts anions (Cl^-, HCO_3^-, SO_4^{2-}) and the MB molecules for the vacant sites on the adsorbents (MBC and MBC–CH). Similarly, it has been reported that the presence of some inorganic salts in solution hindered adsorption of dye molecules on pine cone adsorbent [33]. Fig. 4 showed that the greatest and least effects on MB adsorption were impacted by the presence Na_2SO_4 and NaCl salts in the solution, respectively. This can be explained by the precipitation of sulphate anions on amino groups of chitosan which led to inhibition of the nearness of the active sites on MBC–CH or increase in thickness of the diffusion layer around the MBC–CH surface [34,35].

3.4. Effect of solution pH on MB adsorption

The surface charge of an adsorbent and dissociation of functional groups on its active sites, the degree of ionization and structural changes of dye molecules can be influenced by pH of the solution [36]. A pH 4–12 range was used to study the adsorption mechanism of MB on MBC–CH. Adsorption of MB was enhanced

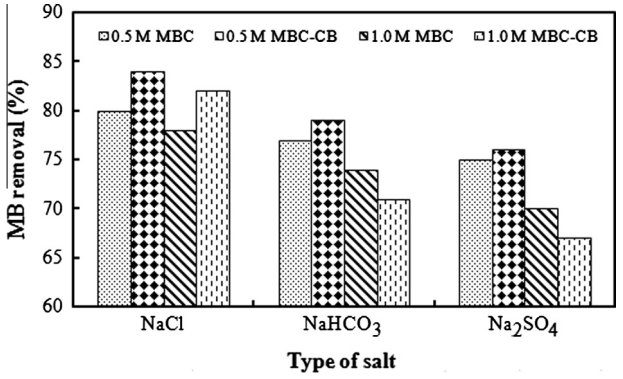

Fig. 4. Effect of inorganic salts on MB adsorption on MBC and MBC–CH (V = 100 mL, W = 0.10 g, shaking speed = 140 rpm, and temperature = 30 °C).

at higher pH of the solution while the reverse was observed as the pH was decreasing; results of effect of pH on MB adsorption by MBC–CH are presented in Fig. 5.

Extinction of positive charges which led to electrostatic attraction between the surface active sites of MBC–CH and the cationic MB molecules was observed as the solution pH was increased due to presence of hydoxls and —COO^- groups. This was contrary to predominance of repulsion activities between MB molecules and protons at lower pH of the solution noticed. Chemical equations of the extinction of positive charge density which increased adsorption of MB on MBC–CH surfaces at elevated pH is given as [25,37]:

$$-SiOH + OH^- \rightleftharpoons -SiO^- + H_2O \quad (9)$$

$$-SiOH + MB^+ \rightarrow -Si-O-MB^+ \quad (10)$$

$$-COO^- + MB^+ \rightarrow -COO^-MB^+ \quad (11)$$

At lower pH of the solution (acidic media), repulsion activities dominated between MB^+ ions and positively charged ($Si-OH^{2+}$) edges groups on the MBC–CH surfaces as represented in the following equation [38]:

$$-SiOH + H^+ \rightarrow -SiOH_2^+ + OH^- \quad (12)$$

3.5. Equilibrium adsorption isotherm studies

An indispensable prerequisite before assessing adsorbent activity in fixed-bed column system is for the sorbent capacity of adsorption for the pollutant to be determined [2]. The adsorption equilibrium isotherm study was used to assess the adsorbent adsorption capacity. Langmuir [39], Freundlich [40] and Redlich–Peterson [41] isotherm models fitting to the experimental data was carried out using their non-linear equations expressed as:

$$q_e = \frac{q_m C_e b}{(1 + bC_e)} \quad (13)$$

$$q_e = K_F C_e^{1/n} \quad (14)$$

where C_e (mg/L) and q_e (mg/g) are the equilibrium concentration and the amount of MB adsorbed, respectively; q_m (mg/g) and b (L/g) are the monolayer adsorption capacity and affinity of MBC–CH towards MB, respectively. The K_F ((mg/g)(L/mg)$^{1/n}$) and n (dimensionless) are the Freundlich constants relaying information on the adsorption extent and degree of nonlinearity between the adsorption and the solution concentration, respectively. Adsorption intensity is evaluated by values of inverse of n (1/n).

$$q_e = \frac{AC_e}{1 + BC_e g} \quad (15)$$

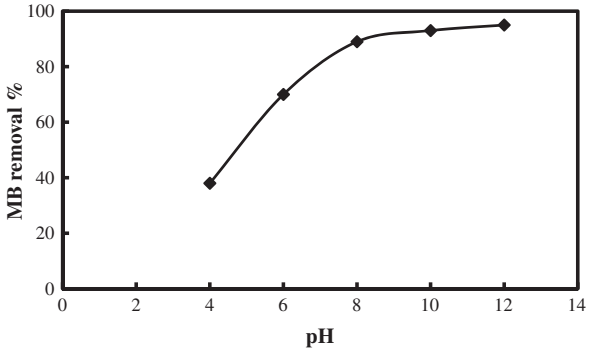

Fig. 5. Effect of solution pH on MB adsorption on MBC–CH (V = 100 mL, W = 0.10 g, shaking speed = 140 rpm, and temperature = 30 °C).

Redlich–Peterson equation (RP) can be linearized by taking natural logarithm of it to give:

$$\ln\left(A\frac{C_e}{q_e} - 1\right) = g\ln(C_e) + \ln(B) \quad (16)$$

Since three unknown parameters A, B, and g are involved in the expression, a trial and error has been developed with the aid of computer application to obtain optimum values of the parameters adjudged by the coefficient of determination, R^2 [42].

The adsorption process was laxly described by Langmuir model even though the correlation coefficient values R^2 of the model results were above 0.800; this is in comparison with the R^2 values of Freundlich and Redlich–Peterson (R–P) values which had least R^2 value of 0.941. High R^2 values of Freundlich isotherm model showed a good fitting of the model to the experimental data; the reciprocal of n values which were less than unity indicated favorability of adsorption of MB on MBC–CH. The models parameters values obtained are summarized in Table 1. Redlich–Peterson isotherm model best described the equilibrium adsorption behavior of MB on MBC–CH, this is similar to report on adsorption of MB by MBC [18]. The R–P model has attributes of both Langmuir and Freundlich isotherms and its parameter (g) values obtained were tending towards zero. Redlich–Peterson model satisfies Langmuir model conditions when its g = 1 and that of Freundlich isotherm when g value is close to zero. It can be said that the order of fitness from the least to the best of MB adsorption on MBC–CH for the isotherm models investigated was Langmuir, Freundlich and Redlich–Peterson. Similar order of fitness has been reported [43].

Comparatively, the monolayer adsorption capacity of MBC–CH for MB was higher than that of MBC [18] by 159%. This was attributed to the use of chitosan for the modification of the MBC adsorbent. Chitosan is composed of both amines and hydroxyl groups but it is predominantly cationic polysaccharide in nature [7]. The presence of the OH^- groups in chitosan biopolymer contributed to its MB adsorption from acqueous solution [44]. The enhancement of dispersion and suspension ability of the MBC clay in acqueous solution by intercalation of cationic chitosan in the structure of the expandable aluminosilicate increased the diffusion of MB molecules into the MBC–CH [8,9].

3.6. Kinetics of MB adsorption on MBC–CH

The kinetic experiment data were modeled by pseudo-first-order [45] and pseudo-second-order kinetic [46] models. The nonlinear expressions of the models are expressed thus:

$$q_t = q_e(1 - e^{-k_1 t}) \quad (17)$$

$$q_t = \frac{k_2 q_e^2 t}{(1 + k_2 q_e t)} \quad (18)$$

where q_e and q_t (mg/g), are the amount of MB adsorbed at equilibrium and at any time t (min), respectively; k_1 (h^{-1}) and k_2 (g/mg h) are the pseudo-first-order and pseudo-second-order rate constants, respectively.

Plots of q_t against t used for the determination of the models parameters gave good curves fittings (figure not shown) and the kinetic results are shown in Table 2. The results revealed that pseudo-second-order model best fitted the adsorption data than pseudo-first-order model. This was observed by higher correlation coefficient R^2 values of the model even though report has it that R^2 value is not sufficient to be used for selection of kinetic model fitting [47]. The Chi-square (χ^2) generated further affirmed the fitness of pseudo-second-order kinetic model to the adsorption data. The Chi-square values of the pseudo-first-order were minimal between 30 and 60 mg/L and suddenly became larger at

Table 1
Langmuir, Freundlich and Redlich–Peterson isotherm models parameters for MB adsorption by MBC–CH.

Isotherms	Parameters	MBC–CH		
		30 °C	40 °C	50 °C
Langmuir	q_m (mg/g)	259.810	264.890	282.700
	b (L/mg)	0.045	0.059	0.020
	R^2	0.894	0.846	0.925
Freundlich	K_F ((mg/g) (L/mg)$^{1/n}$)	13.845	22.927	29.533
	$1/n$	0.558	0.484	0.482
	R^2	0.960	0.941	0.955
Redlich–Peterson	g	0.715	0.198	0.003
	B (L/mg)^g	0.104	2.784	0.006
	A (L/g)	6.868	20.798	3.661
	R^2	0.996	0.986	0.982

Table 2
Kinetic models parameters for MB adsorption by MBC–CH at 30 °C.

MB conc. (mg/L)	q_{exp} (mg/g)	Pseudo-first-order parameters				Pseudo-second-order parameters			
		k_1 (h^{-1})	q_{cal}	χ^2	R^2	k_2 (g/mg h)	q_{cal}	χ^2	R^2
30	26.933	0.128	29.558	0.675	0.974	4.870	33.244	3.190	0.970
60	52.132	0.081	57.147	4.798	0.987	1.470	66.285	3.961	0.990
100	79.764	0.116	80.776	9.966	0.967	1.740	90.361	6.807	0.990
200	135.704	0.089	127.114	13.570	0.942	0.785	148.485	10.887	0.983
300	193.230	0.106	190.470	19.323	0.982	0.629	215.969	7.883	0.998

higher concentration; this further confirmed the assertion that pseudo-first-order kinetics is mostly suitable at short range, especially at the initial stage of the adsorption process. On the contrary, the Chi-square values of the pseudo-second-order model parameters were moderately distributed across a wider range which supports the fact that the mechanism of adsorption was the rate controlling step [48].

3.7. Thermodynamics of adsorption

The adsorption principles of MBC–CH and MB equilibrium surface interaction was studied by adopting Gibb's expression [49]. Temperature variations of 30, 40 and 50 °C were used for the study. The Gibb's free energy (ΔG) of the process was determined using the following equation:

$$\Delta G = -RT \ln K_o \tag{19}$$

And the enthalpy (ΔH) and entropy (ΔS) of the MB adsorption were expressed as:

$$\ln K_o = \frac{\Delta G}{RT} = \frac{\Delta S}{R} - \frac{\Delta H}{RT} \tag{20}$$

where R is the universal gas constant (8.314 J/Kmol); T, absolute temperature (K); K_0 distribution coefficient expressed as $K_0 = C_e$ (adsorbent)/C_e (solution). And from the plot of $\ln K_0$ against $1/T$ (figure not shown), the intercept and slope were used to determine values of ΔH and ΔS, respectively. The thermodynamic adsorption parameters determined are summarized in Table 3.

The positive value of ΔH (30 kJ/mol) revealed that adsorption efficiency increased with an increase in the process temperature; this implies that each MB molecule had to displace more than one water molecule from the adsorbent surface before it is adsorbed [50]. Positive values of ΔS (103.34 J/mol K) obtained showed that there was an affinity between the MB molecules and MBC–CH surface, and the degree of dispersion of the process increased with increase temperature rise.

Adsorption of MB on MBC–CH was spontaneous; this was revealed by the negative Gibbs free energy (ΔG) values (−1.4 to −3.5 kJ/mol) at various temperatures studied. The increase in spontaneity with increase in temperature implies that adsorption of MB on MBC–CH was more favorable at higher temperatures [12].

Table 3
Thermodynamic properties of MB adsorption on MBC–CH.

Adsorbent	ΔH (kJ/mol)	ΔS (kJ/mol)	ΔG (kJ/mol)		
			303 K	313 K	323 K
MBC–CH	29.997	0.103	−1.435	−2.055	−3.468

3.8. Regeneration studies

The regeneration study results are presented in Fig. 6. The MBC–CH composite showed higher resilience than MBC after five regeneration cycles, this was attributed to the synergetic effect of coalesced chitosan and modified Ball clay properties as described in our previous studies [12,18]. The desorption efficiency may have been enhanced by repulsion activities between the MB molecules and protonation of the MBC–CH surface in the stripping solution. This observation is similar to findings reported by previous

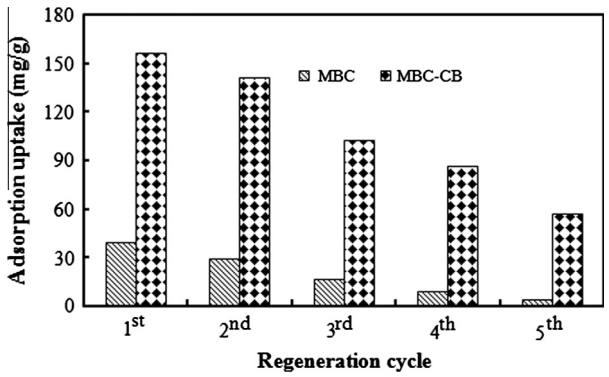

Fig. 6. Regeneration of MBC and MBC–CH after adsorption of MB (V = 100 mL, W = 0.10 g, shaking speed = 140 rpm, and temperature = 30 °C).

researchers on chitosan composites adsorbents [8,51]. The decrease in the adsorption uptake for MB on MBC–CH with increasing regeneration cycles was attributed to the increase in the adsorbate molecules that were strongly attached to the adsorbent surface possibly via chemical adsorption [8].

3.9. Fixed-bed adsorption column study

A perfect design of a real world environmental wastewater purification adsorption column should adequately be guided by detail information on the column operations; this includes the effect of solution flow rate, influent concentration and amount of adsorbent (depth or height) required for each operation.

3.9.1. Effect of initial influent concentration on MB adsorption by MBC and MBC–CH

At a fixed-bed depth of 3.6 cm and a flow rate of 5 mL/min, effect of 50, 100 and 200 mg/L solution concentration on MB adsorption by MBC/MBC–CH was studied. It was observed that the increase in influent concentration was directly proportional to the sorption capacity as shown in Table 4. This was attributed to increase in driving force (concentration gradient or mass transfer) for the adsorption process. The result revealed a percentage increase of 140.12% and 157.53% in sorption capacity for MBC and MBC–CH, respectively when the influent concentration was changed from 50 to 200 mg/L. Similar observation has been reported by previous researchers on increased dye adsorption with increase in initial solution concentration [52]. Comparison of the two adsorbents activities revealed that MBC–CH adsorption capacity was higher than that of MBC by 102.98%. However the increase in influent concentration shortened the breakthrough point while extended breakthrough point was observed at lower concentration as shown in Fig. 7 for MBC and MBC–CH. The extension of breakthrough point in the lower influent concentration was due to lower mass transfer in the adsorption process which leads to the treatment of more volume of MB solution [4].

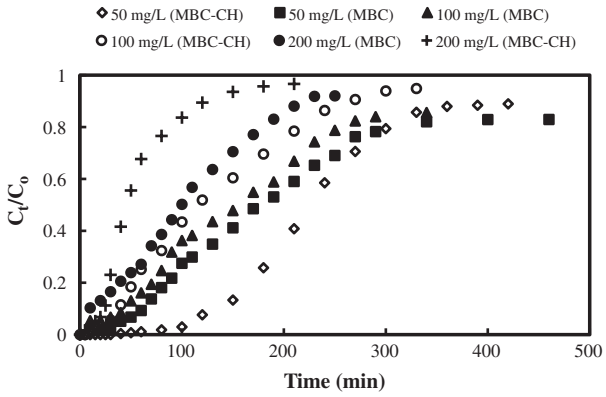

Fig. 7. Effect of concentration on fixed-bed column adsorption of MB by MBC and MBC–CH (flow rate of 5 mL/min, bed depth of 3.6 cm, temperature of 30 °C).

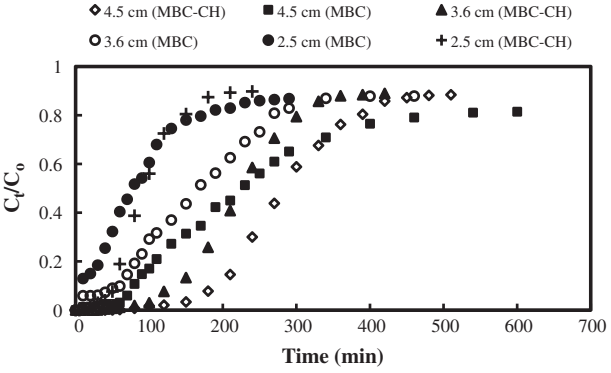

Fig. 8. Effect of bed depth on fixed-bed adsorption of MB adsorption by MBC and MBC–CH (flow rate of 5 mL/min, Initial MB concentration of 50 mg/L, and temperature of 30 °C).

3.9.2. Effect of bed height on adsorption of MB by MBC/MBC–CH

Increase in bed height of adsorption columns leads to an extension of breakthrough point as well as the exhaustion time of adsorbent. This is due to increase in the amount of adsorbent in the column which translates to increase in service area [13]. Axial dispersion is more often dominant over actual expected mass transfer of solute during column adsorption when shorter bed heights used as opposed to longer bed height [53]. Effect of bed height on the fixed-bed adsorption of MB by both adsorbents is shown in Fig. 8. Bed height containing MBC or MBC–CH of 2.5, 3.6 and 4.5 cm for MB adsorption was varied at a fixed flow rate of 5 mL/min and 50 mg/L. It was observed that the sorption capacity and breakthrough time increased with an increase in the bed height as shown in Table 4 and Fig. 8, respectively. This sorption capacity increase can be attributed to sufficient residence time of MB solute in the column adsorption region which provided ample time for diffusion or interaction of the solute molecules with the adsorbent. An increase in adsorption capacity of 25.60–35.31 mg/g and 40.84–58.32 mg/g for MBC and MBC–CH, respectively was recorded. But above all, the sorption capacities of MB on MBC–CH were higher than those of MBC at all bed heights studied.

3.9.3. Effect of influent flow rate on MB adsorption by MBC/MBC–CH

Reduction in exhaustion or column saturation and residence time due to unsatisfactory utilization of adsorption bed is a common phenomenon whenever higher or outrageous flow rates of solution are used in column adsorption processes [54]. An increase in sorption capacity was observed when the solution flow rate was increased from 5 to 8 mL/min for both MBC and MBC–CH adsorption of MB. But at 10 mL/min, the sorption capacity decreased for adsorbents; the results are summarized in Table 4. This was attributed to intense competition for the limited active sites of

Table 4
Fixed-bed column adsorption data of MB by MBC and MBC–CH.

MB influent conc. C_o (mg/L)	Bed depth H (cm)	Flow rate Q (mL/min)	MBC		MBC–CH	
			q_{total} (mg/g)	q_e (mg/g)	q_{total} (mg/g)	q_e (mg/g)
50	2.5	5	30.716	25.597	32.670	40.838
50	3.6	5	58.395	29.198	55.260	55.260
50	4.5	5	112.995	35.311	69.980	58.317
100	3.6	5	86.374	43.187	125.500	125.500
200	3.6	5	140.217	70.109	142.310	142.310
50	3.6	8	134.295	67.148	95.410	95.410
50	3.6	10	122.890	61.445	89.840	89.840

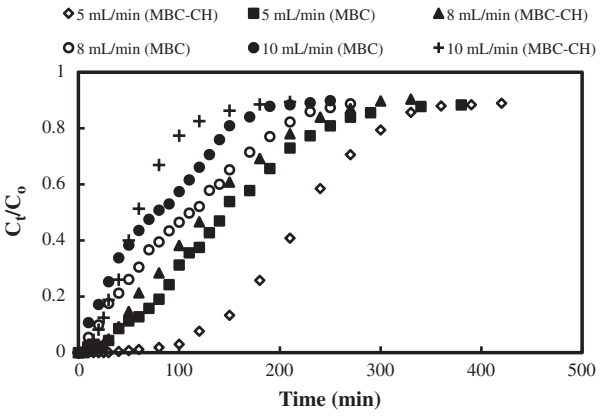

Fig. 9. Effect of influent flow rate on fixed-bed adsorption of MB by MBC and MBC–CH (bed depth of 3.6 cm, Initial MB concentration of 50 mg/L, and temperature of 30 °C).

the adsorbents by the numerous adsorbate molecules present in higher flow of solution. An increase in flow rate of the solution (5–10 mL/min) also led to the shortening of the service time and occurrence of premature breakthrough [55]; this is shown in Fig. 9.

3.10. Bohart–Adams model

Bohart–Adams model which was originally used for gaseous application has been transposed for liquid applications; its suitability is in low concentration regions (much lower than the initial concentration) and when the speed of adsorption is limited by mass transfer [56]. The model's experimental sorption capacity N_o was found to be increasing with increase in concentration but decreasing with increase in solution flow rate for adsorption of MB on both MBC and MBC–CH as shown in Table 5. Also observed on MB adsorption by the two adsorbents is the decrease in mass transfer coefficient k_{BA} with increase in the initial concentration of MB. This is attributed to dominance of external mass transfer activities during adsorption in the column at the initial stages [57].

3.11. Yoon–Nelson model

The results for Yoon–Nelson model parameters for both MBC and MBC–CH adsorbents are shown in Table 6. The time required for 50% breakthrough 'τ' increased with increase in bed height for both adsorbents but was found to decrease with increase in MB concentration only with MBC–CH adsorbent. A similar observation was made during sorption study using Mangostana garcinia peel-based granular activated-carbon [58]. Increase in flow rate from 5 to 10 mL/min led to decrease in τ of MBC–CH, but MBC values of τ decreased 5–8 mL/min. The model rate velocity constant values for MBC did not follow any trend.

The analysis of the applicability of the two dynamic models for prediction of MB adsorption on both MBC and MBC–CH revealed that Bohart–Adams models constants had a pattern of describing the adsorption process as compared with that of Yoon–Nelson model. Also to note was the correlation coefficients R^2 values which between 0.803–0.988 (MBC) and 0.932–0.997 (MBC–CH) for Bohart–Adams model as compared with 0.711–0.902 (MBC) and 0.826–0.896 (MBC–CH) for Yoon–Nelson model MB adsorption data fittings. Adsorption of MB on both MBC and MBC–CH can best be predicted by Bohart–Adams model. That is adsorption rate of MB on both MBC and MBC–CH was proportional to residual capacity of the adsorbents determined at low concentrations or initial part of the breakthrough curves [59].

3.12. Effect of Fixed-bed column adsorption system failure

The failure of the system in the course of the experiment allowed the adsorbent particle to rejuvenate by gradual diffusion of the sorbate molecules into the adsorbent thereby creating ample vacant sites for other molecules. The adsorption system failure profiles for MBC and MBC–CH are shown in Fig. 10. Increase in residence time for the available adsorbate molecules during system failure increased the adsorbents activity. This was observed by the increased volume of wastewater treated and longer time of exhaustion upon resumption of the adsorption process. The result revealed that MBC and MBC–CH activity were not hindered due to the adsorption system failure.

Table 5
Bohart–Adams model parameters of MB adsorption by MBC and MBC–CH.

MB influent conc. C_o (mg/L)	Bed depth H (cm)	Flow rate Q (mL/min)	MBC			MBC–CH		
			k_{BA} (L/mg min) 10^3	N_o (mg/L)	R^2	k_{BA} (L/mg min) 10^3	N_o (mg/L)	R^2
50	2.5	5	0.40	8.964	0.988	2.399	53.598	0.972
50	3.6	5	3.40	13.148	0.977	1.540	80.103	0.981
50	4.5	5	2.20	16.548	0.823	1.078	94.829	0.944
100	3.6	5	1.00	28.714	0.925	0.721	90.425	0.968
200	3.6	5	0.50	41.848	0.902	0.605	94.803	0.983
50	3.6	8	1.80	12.048	0.803	2.379	32.890	0.932
50	3.6	10	1.83	8.382	0.850	1.940	28.538	0.997

Table 6
Yoon–Nelson model parameters of MB adsorption by MBC and MBC–CH.

MB influent conc. C_o (mg/L)	Bed depth H (cm)	Flow rate Q (mL/min)	MBC			MBC–CH		
			k_{YN} (1/min)	τ (min)	R^2	k_{YN} (1/min)	τ (min)	R^2
50	2.5	5	0.006	89.27	0.711	0.037	13.43	0.823
50	3.6	5	0.007	89.59	0.776	0.026	27.07	0.855
50	4.5	5	0.007	100.11	0.865	0.022	34.14	0.878
100	3.6	5	0.006	111.37	0.876	0.021	16.09	0.896
200	3.6	5	0.009	77.08	0.902	0.035	7.60	0.849
50	3.6	8	0.018	30.82	0.887	0.021	16.74	0.864
50	3.6	10	0.005	102.98	0.875	0.029	9.33	0.826

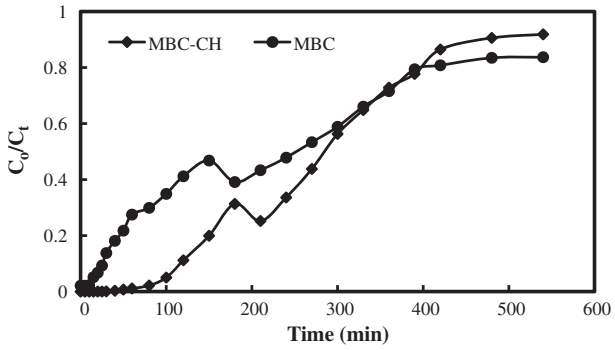

Fig. 10. Effect of adsorption system failure on breakthrough curve for MB uptake by MBC and MBC–CH (bed depth of 3.6 cm, Initial MB concentration of 50 mg/L, flow rate of 5 mL/min, and temperature of 30 °C).

4. Conclusion

Modified Ball clay (MBC) chitosan composite (MBC–CH) adsorbent was successfully prepared and used for adsorption of methylene blue (MB). The adsorption capacity of MB on MBC–CH was higher than that of MBC by 159 %. Adsorption of MB on MBC–CH was found to increase as the initial concentration, solution pH and temperation of the process were increased. The presence of sodium sulfate anions in the solution had greater MB adsorption inhibition on both MBC and MBC–CH than the bicarbonate and chloride anions of sodium salts studied. Investigation of fitness of dynamic adsorption models to the experimental data revealed that Bohart–Adams dynamic model best described the process than the Yoon–Nelson as exhibited by the higher R^2 values and trend of the model's parameters. The degree of randomness of the MB adsorption on MBC–CH was found to be increasing with increase in the process temperature which was thermodynamically spontaneous and endothermic. The MBC–CH showed higher resilience than MBC on the adsorption efficiency after five regeneration cycles. This revealed that MB in aqueous solution can be adsorbed effectively using MBC–CH a number of times before discarded.

Acknowledgement

Authors acknowledge the research grant provided by the Universiti Sains Malaysia under the Postgraduate Research Grant Scheme (PRGS) (Project No. 1001/PJKIMIA/8045026).

References

[1] R. Marandi, Biosorption of hexavalent chromium from aqueous solution by dead fungal biomass of phanerochaete crysosporium: batch and fixed bed studies, Can. J. Chem. Eng. Technol. 2 (2011) 8–22.
[2] Y.S. Al-Degs, M.A.M. Khraisheh, S.J. Allen, M.N. Ahmad, Adsorption characteristics of reactive dyes in columns of activated carbon, J. Hazard. Mater. 165 (2009) 944–949.
[3] E.I. Unuabonah, B.I. Olu-Owolabi, E.I. Fasuyi, K.O. Adebowale, Modeling of fixed-bed column studies for the adsorption of cadmium onto novel polymer–clay composite adsorbent, J. Hazard. Mater. 179 (2010) 415–423.
[4] E. Malkoc, Y. Nuhoglu, Fixed bed studies for the sorption of chromium(VI) onto tea factory waste, Chem. Eng. Sci. 61 (2006) 4363–4372.
[5] S.K. Maji, Y.-H. Kao, C.-J. Wang, G.-S. Lu, J.-J. Wu, C.-W. Liu, Fixed bed adsorption of As(III) on iron-oxide-coated natural rock (IOCNR) and application to real arsenic-bearing groundwater, Chem. Eng. J. 203 (2012) 285–293.
[6] A. Santhana Krishna Kumar, R. Ramachandran, S. Kalidhasan, V. Rajesh, N. Rajesh, Potential application of dodecylamine modified sodium montmorillonite as an effective adsorbent for hexavalent chromium, Chem. Eng. J. 211-212 (2012) 396–405.
[7] J. Johns, V. Rao, Adsorption of methylene blue onto natural rubber/chitosan blends, Int. J. Polym. Mater. 60 (2011) 766–775.
[8] L. Wang, J. Zhang, A. Wang, Fast removal of methylene blue from aqueous solution by adsorption onto chitosan-g-poly(acrylic acid)/attapulgite composite, Desalination 266 (2011) 33–39.
[9] S.M.L. Silva, C.R.C. Braga, M.V.L. Fook, C.M.O. Raposos, L.H. Carvalho, E.L. Canedo, Application of infrared spectroscopy to analysis of chitosan clay nanocomposites infrared spectroscopy, in: T. Theophile (Ed.), Materials Science, Engineering and Technology, In Tech, Europe (2012) 43–63.
[10] M.-Y. Chang, R.-S. Juang, Adsorption of tannic acid, humic acid, and dyes from water using the composite of chitosan and activated clay, J. Colloid Interf. Sci. 278 (2004) 18–25.
[11] M. Rabiul Awual, M. Ismael, T. Yaita, S.A. El-Safty, H. Shiwaku, Y. Okamoto, S. Suzuki, Trace copper(II) ions detection and removal from water using novel ligand modified composite adsorbent, Chem. Eng. J. 222 (2013) 67–76.
[12] M. Auta, B.H. Hameed, Coalesced chitosan activated carbon composite for batch and fixed-bed adsorption of cationic and anionic dyes, Colloids Surface B, Biointerf. 105 (2013) 199–206.
[13] I.A.W. Tan, A.L. Ahmad, B.H. Hameed, Adsorption of basic dye using activated carbon prepared from oil palm shell: batch and fixed bed studies, Desalination 225 (2008) 13–28.
[14] V.K. Gupta, Suhas, Application of low-cost adsorbents for dye removal – a review, J. Environ. Manage. 90 (2009) 2313–2342.
[15] A. Demirbas, Agricultural based activated carbons for the removal of dyes from aqueous solutions: a review, J. Hazard. Mater. 167 (2009) 1–9.
[16] Y. Liu, Y. Zheng, A. Wang, Enhanced adsorption of methylene blue from aqueous solution by chitosan-g-poly(acrylic acid)/vermiculite hydrogel composites, J. Environ. Sci. 22 (2010) 486–493.
[17] M. Rafatullah, O. Sulaiman, R. Hashim, A. Ahmad, Adsorption of methylene blue on low-cost adsorbents: a review, J. Hazard. Mater. 177 (2010) 70–80.
[18] M. Auta, B.H. Hameed, Modified mesoporous clay adsorbent for adsorption isotherm and kinetics of methylene blue, Chem. Eng. J. 198–199 (2012) 219–227.
[19] D.S. Faust, M.O. Aly, Adsorption Processes for Water Treatment, Butterworth Publishers (1987).
[20] E. Malkoc, Y. Nuhoglu, Y. Abali, Cr(VI) adsorption by waste acorn of quercus ithaburensis in fixed beds: prediction of breakthrough curves, Chem. Eng. J. 119 (2006) 61–68.
[21] Z. Aksu, F. Gönen, Biosorption of phenol by immobilized activated sludge in a continuous packed bed: prediction of breakthrough curves, Process Biochem. 39 (2004) 599–613.
[22] K.H. Chu, Fixed bed sorption: setting the record straight on the Bohart–Adams and Thomas models, J. Hazard. Mater. 177 (2010) 1006–1012.
[23] Y.H. Yoon, J.H. Nelson, Application of gas adsorption kinetics. I. A theoretical model for respirator cartridge service life, Am. Ind. Hyg. Assoc. J. 45 (1984) 509–516.
[24] A. Casariego, B.W.S. Souza, M.A. Cerqueira, J.A. Teixeira, L. Cruz, R. Díaz, A.A. Vicente, Chitosan/clay films' properties as affected by biopolymer and clay micro/nanoparticles' concentrations, Food Hydrocolloid 23 (2009) 1895–1902.
[25] L. Fan, C. Luo, M. Sun, X. Li, F. Lu, H. Qiu, Preparation of novel magnetic chitosan/graphene oxide composite as effective adsorbents toward methylene blue, Biores. Technol. 114 (2012) 703–706.
[26] N.K. Lazaridis, G.Z. Kyzas, A.A. Vassiliou, D.N. Bikiaris, Chitosan derivatives as biosorbents for basic dyes, Langmuir 23 (2007) 7634–7643.
[27] J. Madejová, FTIR techniques in clay mineral studies, Vib. Spectrosc. 31 (2003) 1–10.
[28] C.D. Tran, S. Duri, A. Delneri, M. Franko, Chitosan–cellulose composite materials: preparation, characterization and application for removal of microcystin, J. Hazard. Mater. 252–253 (2013) 355–366.
[29] L.W. Low, T.T. Teng, A. Ahmad, N. Morad, Y.S. Wong, A novel pretreatment method of lignocellulosic material as adsorbent and kinetic study of dye waste adsorption, Water Air Soil Pollut. 218 (2010) 293–306.
[30] K.L. Konan, C. Peyratout, A. Smith, J.P. Bonnet, S. Rossignol, S. Oyetola, Comparison of surface properties between kaolin and metakaolin in concentrated lime solutions, J. Colloid Interf. Sci. 339 (2009) 103–109.
[31] N. Nasuha ∗, B.H. Hameed, Azam T. Mohd Din, Rejected tea as a potential low-cost adsorbent for the removal of methylene blue, J. Hazard. Mater. 175 (2010) 126–132.
[32] M. Auta, B.H. Hameed, Optimized waste tea activated carbon for adsorption of methylene blue and acid blue 29 dyes using response surface methodology, Chem. Eng. J. 175 (2011) 233–243.
[33] N.M. Mahmoodi, B. Hayati, M. Arami, C. Lan, Adsorption of textile dyes on Pine Cone from colored wastewater: kinetic, equilibrium and thermodynamic studies, Desalination 268 (2011) 117–125.
[34] R. Salehi, M. Arami, N.M. Mahmoodi, H. Bahrami, S. Khorramfar, Novel biocompatible composite (chitosan–zinc oxide nanoparticle): preparation, characterization and dye adsorption properties, Colloids Surf. B: Biointerf. 80 (2010) 86–93.
[35] G.O. El-Sayed, Removal of methylene blue and crystal violet from aqueous solutions by palm kernel fiber, Desalination 272 (2011) 225–232.
[36] L. Wang, J. Zhang, R. Zhao, C. Li, Y. Li, C. Zhang, Adsorption of basic dyes on activated carbon prepared from polygonum orientale Linn: Equilibrium, kinetic and thermodynamic studies, Desalination 254 (2010) 68–74.
[37] A.S. ALzaydien, Adsorption of methylene blue from aqueous solution onto a low-cost natural jordanian tripoli, Am J. Environ. Sci. 5 (2009) 197–208.
[38] B.A. Fil, C. Özmetin, M. Korkmaz, Cationic dye (methylene blue) removal from aqueous solution by montmorillonite, Bull. Kor. Chem. Soc. 33 (2012) 3184–3190.
[39] I. Langmuir, The constitution and fundamental properties of solids and liquids, J. Am. Chem. Soc. 38 (1916) 2221–2295.

[40] H.M.F. Freundlich, Over the adsorption in solution, J. Phys. Chem. 57 (1906) 385–470.
[41] O. Redlich, D.L. Peterson, A useful adsorption isotherm, J. Phy. Chem. 63 (1959) 1024.
[42] Y.-S. Ho, W.-T. Chiu, C.-C. Wang, Regression analysis for the sorption isotherms of basic dyes on sugarcane dust, Bioresour. Technol. 96 (2005) 1285–1291.
[43] J. Yang, K. Qiu, Preparation of activated carbons from walnut shells via vacuum chemical activation and their application for methylene blue removal, Chem. Eng. J. 165 (2010) 209–217.
[44] V.M. Boddu, K. Abburi, J.L. Talbott, E.D. Smith, Removal of hexavalent chromium from wastewater using a new composite chitosan biosorbent, Environ. Sci. Technol. 37 (2003) 4449–4456.
[45] S. Lagergren, B.K. Svenska, On the theory of so-called adsorption of dissolved substances, The Royal Swed Acad Sci Doc Band 24 (1898) 1–13.
[46] Y.S. Ho, G. McKay, Pseudo-second order model for sorption processes, Process Biochem. 34 (1999) 451–465.
[47] S. Azizian, B. Yahyaei, Adsorption of 18-crown-6 from aqueous solution on granular activated carbon: a kinetic modeling study, J. Colloid Interface Sci. 299 (2006) 112–115.
[48] Y.S. Ho, G. McKay, Sorption of dye from aqueous solution by peat, Chem. Eng. J. 70 (1998) 115–124.
[49] M.D. Ruthven, Principles of Adsorption & Adsorption Processes, John wiley and sons, New York, 1984.
[50] D. Kołodyńska, R. Wnętrzak, J.J. Leahy, M.H.B. Hayes, W. Kwapiński, Z. Hubicki, Kinetic and adsorptive characterization of biochar in metal ions removal, Chem. Eng. J. 197 (2012) 295–305.
[51] W.S. Wan Ngah, N.F.M. Ariff, A. Hashim, M.A.K.M. Hanafiah, Malachite green adsorption onto chitosan coated bentonite beads: isotherms, Kinet Mech Clean – Soil, Air, Water 38 (2010) 394–400.
[52] A. Goshadrou, A. Moheb, Continuous fixed bed adsorption of C.I. acid blue 92 by exfoliated graphite: an experimental and modeling study, Desalination 269 (2011) 170–176.
[53] V.C. Taty-Costodes, H. Fauduet, C. Porte, Y.-S. Ho, Removal of lead (II) ions from synthetic and real effluents using immobilized *Pinus sylvestris* sawdust: adsorption on a fixed-bed column, J. Hazard. Mater. 123 (2005) 135–144.
[54] S. Hussain, H.A. Aziz, M.H. Isa, A. Ahmad, J. Van Leeuwen, L. Zou, S. Beecham, M. Umar, Orthophosphate removal from domestic wastewater using limestone and granular activated carbon, Desalination 271 (2011) 265–272.
[55] X. Wu, D. Wu, R. Fu, W. Zeng, Preparation of carbon aerogels with different pore structures and their fixed bed adsorption properties for dye removal, Dyes Pigm. 95 (2012) 689–694.
[56] A. Ghribi, M. Chlendi, Modelling of fixed bed adsorptio: application to the adsorption of organic dye, Asian J. Text. 1 (2011) 161–171.
[57] Z.Z. Chowdhury, S.M. Zain, A.K. Rashid, R.F. Rafique, K. Khalid, Breakthrough curve analysis for column dynamics sorption of Mn(II) ions from wastewater by using mangostana garcinia peel-based granular-activated carbon, J. chem. 2013 (2013) 1–8.
[58] A.A. Ahmad, B.H. Hameed, Fixed-bed adsorption of reactive azo dye onto granular activated carbon prepared from waste, J. Hazard. Mater. 175 (2010) 298–303.
[59] M. Trgo, N.V. Medvidovic, J. Peric, Application of mathematical empirical models to dynamic removal of lead on natural zeolite clinoptilolite in fixed bed columns, Indian J. Chem. Technol. 18 (2011) 123–131.